Available online at www.sciencedirect.com
ScienceDirect
Current Applied Physics 7 (2007) 51–59
Current Applied Physics
An official journal of the KPS
www.elsevier.com/locate/cap
www.kps.or.kr

Characterization on electron beam evaporated α-MoO_3 thin films by the influence of substrate temperature

R. Sivakumar [a], R. Gopalakrishnan [c], M. Jayachandran [b], C. Sanjeeviraja [a,*]

[a] Department of Physics, Alagappa University, Karaikudi 630 003, India
[b] ECMS Division, Central Electrochemical Research Institute, Karaikudi 630 006, India
[c] Department of Physics, Anna University, Chennai 600 025, India

Received 8 September 2005; received in revised form 3 October 2005; accepted 11 October 2005
Available online 21 November 2005

Abstract

Electrochromic molybdenum oxide (MoO_3) thin films were prepared by electron beam evaporation technique using the dry MoO_3 pellets. The films were deposited on glass and fluorine doped tin oxide (SnO_2:F or FTO) coated glass substrates at different substrate temperatures like room temperature (RT, 30 °C), 100 °C and 200 °C. The influence of substrate temperature on the structural, surface morphological and optical properties of the films has been studied. The X-ray diffraction analysis showed that the films are having orthorhombic phase MoO_3 (α-MoO_3) with ⟨1 1 0⟩ preferred orientation. The laser Raman scattering spectrum shows the polycrystalline nature of MoO_3 films deposited at 200 °C. The Raman-active band at 993 cm^{-1} is corresponding to Mo–O stretching mode that is associated with the unique character of the layered structure of orthorhombic MoO_3. Needle—like morphology was observed from the SEM analysis. The energy band gap of MoO_3 films was evaluated which lies between 2.8 and 2.3 eV depending on the substrate temperature and substrates. The decrease in band gap value with increasing substrate temperature is owing to the oxygen-ion vacancies. The absorption edge shift shows the coloration effect on the films.

PACS: 68.55; 64.70.F; 68.65; 61.40; 32.20.F; 51.70

Keywords: Molybdenum oxide; Thin films; Evaporation; Crystallization; Layer structures; Optical properties

1. Introduction

The transition-metal oxides constitute a very interesting group of semiconducting materials because of their technological applications in the field of display devices [1], optical smart windows, low-refractive materials in filters, low cost electrochromic devices (ECD) [2] and gas-sensors [3]. The various transition-metal oxides are MoO_3, WO_3, V_2O_5, NiO, IrO_2, etc. Among them molybdenum oxide (MoO_3) and tungsten oxide (WO_3), form a group of predominately ionic solids that exhibit electrochromic effect [4]. The electrochromic effect can be described as the reversible change in transmittance and/or reflectance, caused by the application of an externally applied trigger (voltage). The electrochromic response of molybdenum oxide is aesthetically superior to many other electrochromic materials (transition-metal oxides), because it absorbs light more intensely and uniformly [4]. Based on the above criteria, in the present work we have attempted to study the molybdenum oxide (MoO_3) thin films for electrochromic devices.

Moreover, the MoO_3 films can be used as a potential electro-active material for high energy density secondary lithium batteries [5,6], because it exhibits two dimensional van der Waals bonded layered structure in orthorhombic phase (α-phase). The orthorhombic phase molybdenum oxide (α-MoO_3) film, has a layered structure comprising of double layers of MoO_6 octahedra held together by two

* Corresponding author. Tel.: +91 4565 230251; fax: +91 4565 225202/230251.
E-mail addresses: krsivakumar1979@yahoo.com (R. Sivakumar), sanjeeviraja@rediffmail.com (C. Sanjeeviraja).

1567-1739/$ - see front matter © 2005 Elsevier B.V. All rights reserved.
doi:10.1016/j.cap.2005.10.001

different covalent forces in the '*a*'- and '*c*'-axes, i.e., ⟨1 0 0⟩ and ⟨0 0 1⟩ directions, but by van der Waals forces in the '*b*'-axis alone, i.e., ⟨0 1 0⟩ direction. The main consequence of this fact is that large MoO_3 crystallites have elongated slab-like nature, preferentially exposing the ⟨0 1 0⟩ direction [7,8].

Now-a-days various techniques are available for the preparation of MoO_3 films with amorphous and crystalline nature on different media (substrates). Generally they are classified into two categories, viz., chemical and physical vapour methods. Chemical methods include different techniques, sol–gel process [9], electrodeposition [10]. Physical methods include thermal evaporation [11], sputtering [12] and electron beam evaporation [13]. However, the device performance is basically related to the structure, morphological, optical and compositional properties of the films which in turn invariably depends on the deposition technique and deposition parameters used for the growth of thin films. Even though, the production cost of the films in the physical vapour deposition technique is high (than the chemical methods), they impart some feasible device based qualities like optimum stoichiometry, morphology and crystalline alignment to the films, which are the key factors deciding the performance of the films for their suitability in developing special devices. For this reason, in the present investigation we have chosen one of the physical vapour deposition methods i.e., the electron beam evaporation technique (PVD:EBE) for the preparation of MoO_3 thin films and optimized the growth conditions with suitable microstructure to enhance the optical coloration effect. The effect of substrate temperature on structural, surface morphological and optical properties of the films are elaborately studied and presented here.

2. Experimental

Thin films of α-MoO_3 were prepared by electron beam evaporation technique using a HINDHIVAC vacuum coating unit (Model: 12A4D) with electron beam power supply (Model: EBG-PS-3K). The films were grown on both microscopic glass and FTO coated glass (with a sheet resistance of about 15 Ω/sq) substrates. Before the deposition of MoO_3 films on FTO substrates, the preparative conditions were optimized for the glass substrates. The dry MoO_3 powder (99.99%) was made into pellets, taken in a graphite crucible and kept on the water-cooled copper hearth of the electron gun. The samples of the palletized MoO_3 targets were heated by means of electron beam collimated from the d.c heated cathode of tungsten filament. The surface of the pellets was scanned by 180° deflected electron beam with an accelerating voltage of 5 kV and a power density of about 1.5 kW/cm^2. The evaporated materials from MoO_3 pellet were deposited as thin films on the substrates in a pressure of about 1×10^{-5} mbar. Continuous rotation of the substrates during the deposition process facilitated the formation of homogeneous and uniform films on the substrate surface. The deposition was carried out at different substrate temperatures (T_{sub}), i.e., RT, 100 °C and 200 °C.

The structural properties of the films were characterized by the JEOL JDX X-ray diffractometer (XRD) with CuKα radiation ($\lambda = 1.5418$ Å). The Raman spectra were recorded on a JASCO NR-1000 laser Raman spectrometer. An Ar-ion laser was tuned to the 514.5 nm line for excitation. The laser power was set at 150–200 mW. The data were stored on a computer and used for peak-shape analysis. Surface morphology of the films was studied by JEOL JSM-5610 LV (Japan) scanning electron microscope (SEM). The optical properties of the films were analyzed by using HITACHI-3400 UV–Vis-NIR spectrophotometer in the wavelength range 300–1100 nm.

3. Results and discussion

3.1. Structural studies

Thin films of MoO_3, prepared at different substrate temperatures, were observed to be well adherent to the substrates and to possess smooth and uniform surfaces. The crystalline nature and phases of the films were studied by the X-ray diffraction analysis. The XRD patterns of MoO_3 films deposited at different substrate temperatures on glass and FTO substrates are shown in Figs. 1 and 2, respectively. The pattern of MoO_3 film on glass substrate at room temperature (T_{sub} = RT) (Fig. 1(a)) shows amorphous nature. This may be attributed to the fact that crystallization of MoO_3 thin films and their crystal lattice orientation are not initiated on the amorphous glass substrates at room temperature. When the films were deposited at higher substrate temperatures say $T_{sub} = 100$ and 200 °C, the crystalline nature of the films are observed to be enhanced, owing to the perfect growth alignment of MoO_3 particles on the substrates. The XRD pattern of the film deposited at 100 °C (Fig. 1(b)) shows few diffraction peaks with very weak intensity. Evidently at this substrate temperature (i.e., $T_{sub} = 100$ °C), the film consists of very small crystallites and particles that are spread on the substrate. This clearly shows that the process of crystallization of MoO_3 films needs higher temperature when deposited on amorphous substrates. When the substrate temperature is further increased beyond 100 °C, we obtained sharp XRD peaks with increased peak intensities. The respective XRD pattern is shown in Fig. 1(c) for the MoO_3 film deposited at $T_{sub} = 200$ °C. These observations reveal that even on amorphous substrates, well crystallized and preferentially oriented films can be deposited by raising the substrate temperature during evaporation.

Even though the substrate temperature is low, i.e., T_{sub} = RT, polycrystalline MoO_3 film was formed on the FTO substrate as observed from the sharp XRD peaks (Fig. 2(a)). The XRD patterns of the films prepared at $T_{sub} = 100$ and 200 °C are shown in Fig. 2(b) and (c), respectively. They are having well oriented sharp peaks, which indicate the crystallinity of MoO_3 films. The crystal-

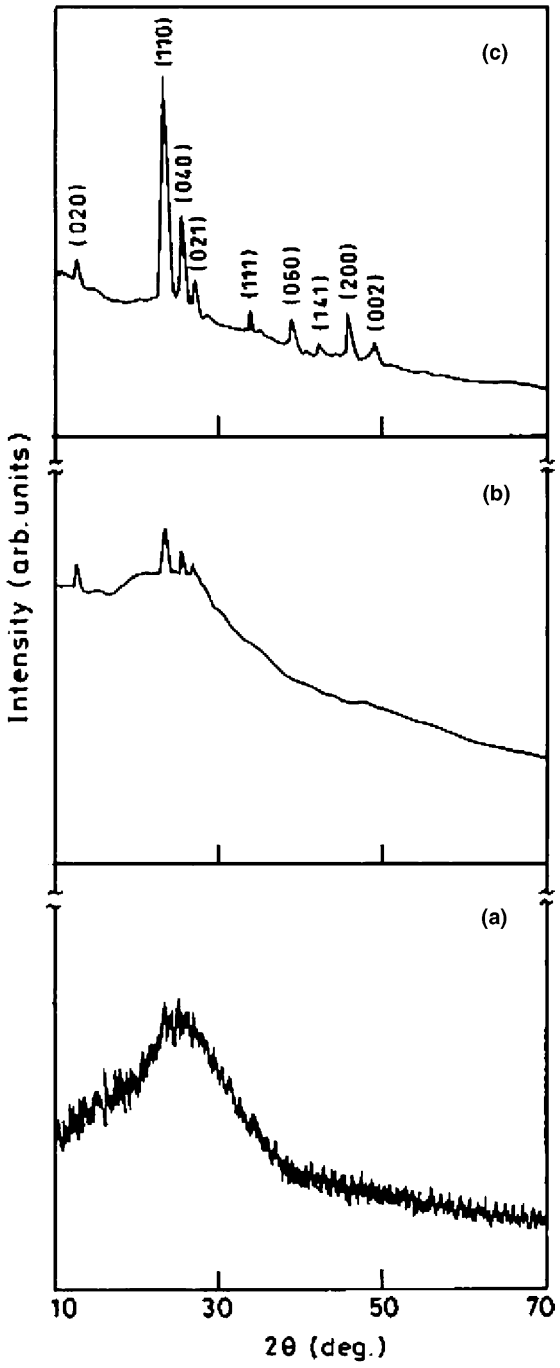

Fig. 1. X-ray diffraction pattern of MoO_3 films on glass substrate at different substrate temperatures: (a) $T_{sub} = RT$, (b) $T_{sub} = 100$ °C and (c) $T_{sub} = 200$ °C.

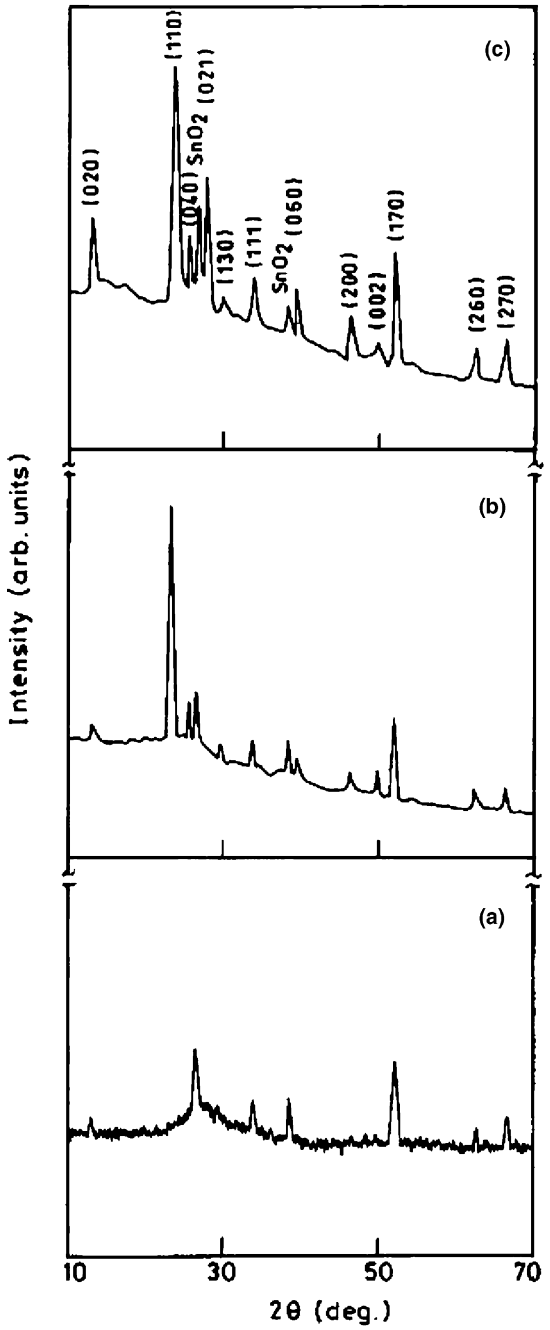

Fig. 2. X-ray diffraction pattern of MoO_3 films on SnO_2:F substrate at different substrate temperatures: (a) $T_{sub} = RT$, (b) $T_{sub} = 100$ °C and (c) $T_{sub} = 200$ °C.

line FTO substrate promotes specific alignment of the arriving atoms and enhances the crystallinity of the films. The observed interplanar distances (d_{hkl}) were compared with the JCPDS (card no. 05-0508) d_{hkl} values. In the present work, the XRD peaks of the MoO_3 films have very good agreement with those of the bulk MoO_3 polycrystalline powder. However, the relative intensity at each observed peak of the MoO_3 films are some what different from the corresponding peaks of the bulk MoO_3 powder.

The relative intensity of the $\langle 110 \rangle$ peak has been found drastically increased in the present work compared to the $\langle 021 \rangle$ peak of maximum intensity for the bulk MoO_3 powder. A close analysis of the XRD results indicates that electron beam evaporated MoO_3 films preferentially grow along $\langle 110 \rangle$ direction. In addition, the presence of well marked peaks like $\langle 020 \rangle$, $\langle 040 \rangle$ and $\langle 060 \rangle$ reveals that the MoO_3 films have some planes grown along $\langle 0k0 \rangle$ i.e., '*b*'-axis ($k = 2$, 4 and 6), which means the stocking of layers one over the other. The presence of $\langle 110 \rangle$, $\langle 130 \rangle$, $\langle 170 \rangle$,

$\langle 260\rangle$ and $\langle 270\rangle$ planes, observed in MoO_3 films deposited on FTO substrates, correspond to the formation of platelets growing along the $\langle hk0\rangle$ direction [7,8]. Such arrangement of crystalline planes and preferred growth of the films enumerates the layered nature of the molybdenum oxide (α-MoO_3) films with orthorhombic phase. The preferential orientation of these films is due to adsorption and accommodation of the impinging atoms with respect to growth parameters and in particular to the nature of substrates. The initial orientation is then followed by the preferred growth of clustering of atoms, which continuously leads to the preferential growth of films on substrates. The requirement for preferential orientation is that this particular orientation should give lower interfacial energy and much high nucleation rate.

The effect of substrate temperature on the degree of crystallinity of the films is clearly demonstrated from the X-ray diffractograms. It is observed that the onset of crystallization in MoO_3 films starts at low deposition temperatures, i.e., $T_{sub} = RT$ and 100 °C for the FTO and glass substrates, respectively. This may be due to the increased kinetic energy of the ionized species or neutral aggregates, which enhances the adatom mobility on the substrate surface [14]. Other aspect is that the grain size of the films

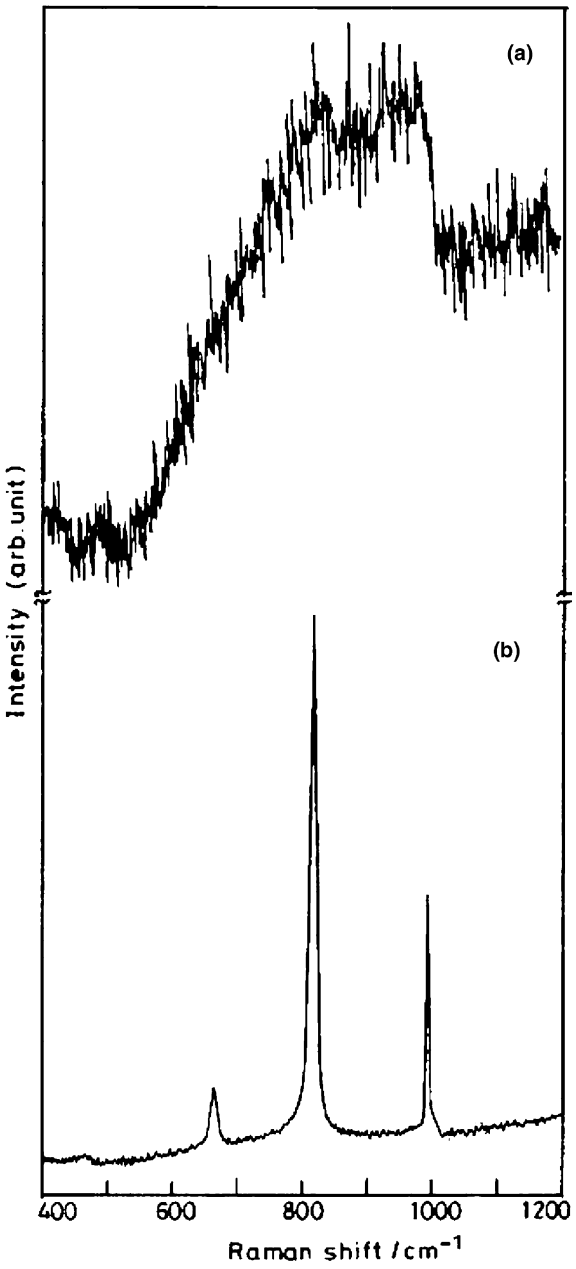

Fig. 3. Raman scattering spectra of MoO_3 films deposited on glass substrates, (a) $T_{sub} = RT$, (b) $T_{sub} = 200$ °C.

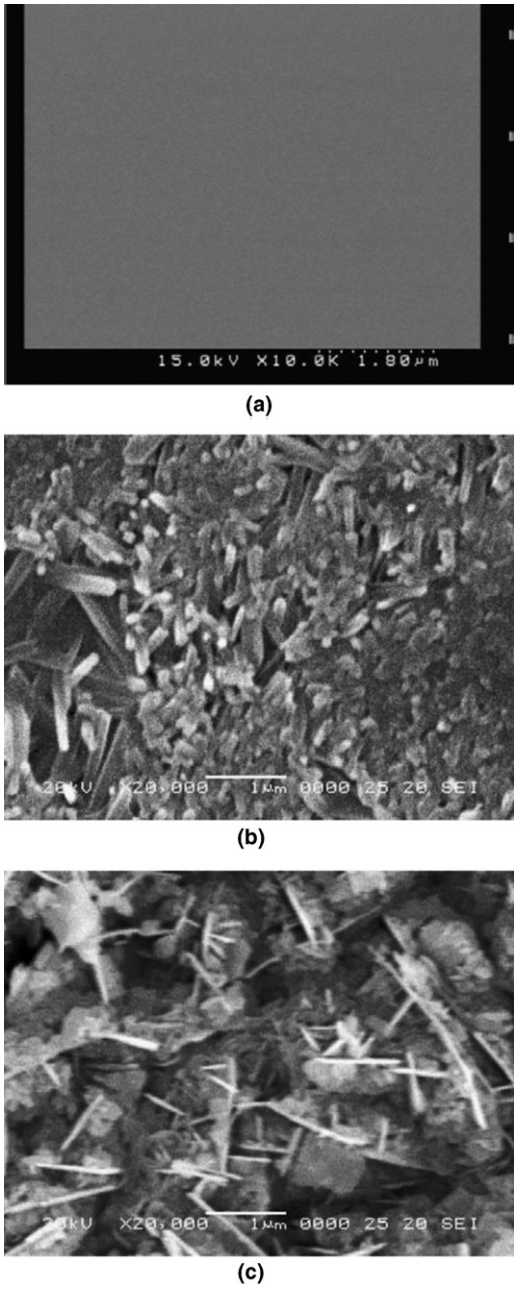

Fig. 4. Surface morphology of MoO_3 films on glass substrate at different substrate temperatures: (a) $T_{sub} = RT$, (b) $T_{sub} = 100$ °C and (c) $T_{sub} = 200$ °C.

increases with increasing substrate temperatures. At higher deposition temperatures, the atomic, molecular or ionic species of MoO_3 impinged on the substrate surface acquire a large thermal energy and hence a large mobility. As a result, a large number of nucleus are formed which coalesce at elevated temperature to form a continuous film with large grains on the substrate [15]. Thus, it is found that the critical parameters determining the quality of thin films varies with the substrate materials and substrate temperatures at which the films are deposited. Abdellaoui et al. [16] reported the orthorhombic phase of MoO_3 with preferred growth along $\langle 1\,1\,0\rangle$ plane for the films annealed at elevated temperatures like 500 and 600 °C in different environments. The orthorhombic symmetry of MoO_3 was reported earlier [17] for the films deposited by spray pyrolysis technique at 300 °C. It can be concluded that, crystalline α-MoO_3 thin films have been prepared by the electron beam evaporation technique even at lower substrate temperatures. High intense and sharp peaks observed in the XRD patterns further confirm the highly oriented and polycrystalline nature of the films.

The calculated values of lattice parameters are $a = 3.964$ Å, $b = 13.852$ Å and $c = 3.698$ Å, which are in good agreement with JCPDS data. The crystallite size of the films, calculated from the Scherrer's formula [18], is of the order of 70 nm, which confirms the presence of nanocrystallites in the MoO_3 films prepared in the present work.

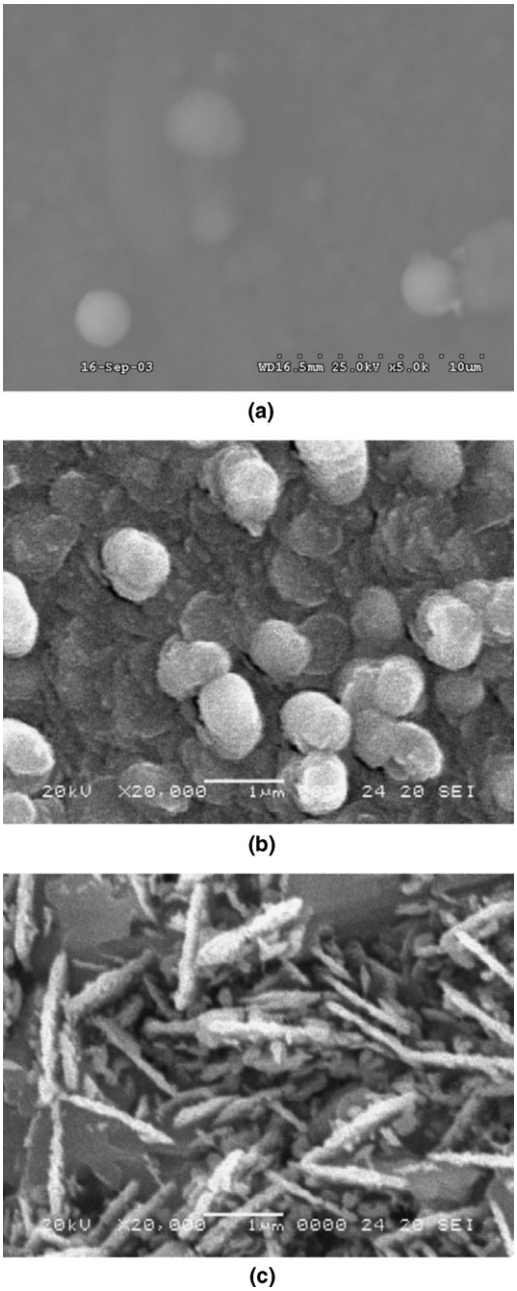

Fig. 5. Surface morphology of MoO_3 films on SnO_2:F substrate at different substrate temperatures: (a) T_{sub} = RT, (b) $T_{sub} = 100$ °C and (c) $T_{sub} = 200$ °C.

3.2. Raman spectroscopic study

Fig. 3 shows laser Raman scattering spectra of the MoO_3 films deposited on glass substrates. The observed Raman spectra of MoO_3 films agree well with the bonding assignments of single crystal MoO_3 studied by using Raman polarized spectroscopy [19]. Beattie and Gilson [20] have made on attempt to apply group frequency assignments to the vibrational spectra of oxides such as MoO_3, V_2O_5, Nb_2O_5 and etc. With MoO_3, the terminal oxygens (OMo), two-connected bridging oxygens (OMo_2)

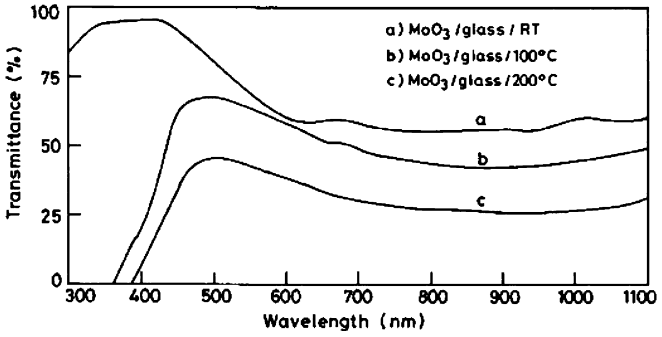

Fig. 6. Optical transmittance spectrum of MoO_3 films on glass substrate at different substrate temperatures.

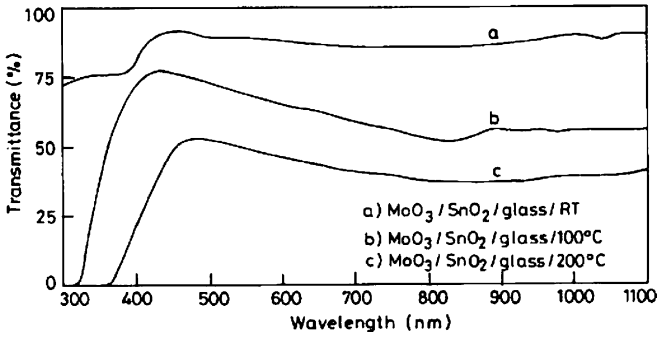

Fig. 7. Optical transmittance spectrum of MoO_3 films on SnO_2:F substrate at different substrate temperatures.

and three-connected bridging oxygens (OMo_3) were considered on the basis of a site symmetry.

The laser Raman scattering spectrum of MoO_3 film deposited at 30 °C (Fig. 3(a)) shows that these films have a rather amorphous structure. From the shape of the Raman spectrum of MoO_3 films, the phonon density of states was observed and it suggests that the structure of the films is amorphous-like. This also correlates with our X-ray diffraction analysis (Fig. 1(a)). The spectrum of higher temperature ($T_{sub} = 200$ °C) produced MoO_3 film corresponds to a thoroughly crystalline structure (Fig. 3(b)). The Raman-active band at about 993 cm^{-1} is corresponding to the stretching mode of the Mo–O and this peak associated with the unique molybdenyl bond (the shortest Mo=O of the structure), which is responsible for the layered structure of α-MoO_3. The bridging oxygens (OMo_2) correspond to Mo–O–Mo, which is corresponding to the bond at 817 cm^{-1}. The vibrational mode corresponding to 665 cm^{-1} is assigned to the stretching of the bridging oxygens of OMo_3. A similar position of these Raman peaks was reported by several authors [19,21] for the orthorhombic modification of MoO_3. Julien et al. [23] reported clearly that the observation of peak at 995 cm^{-1} responsible for the layered structure of α-MoO_3. Thus it may be concluded that all the structural investigations on MoO_3 films converge towards similar results, describing the layered nature of films deposited at substrate temperature of 200 °C.

3.3. Surface analysis

The surface morphological studies of the films were analyzed by JEOL JSM-5610 LV (Japan) scanning electron microscope. Surface microstructure images of MoO_3 films on glass and FTO substrates at $T_{sub} = RT$, 100 and 200 °C are shown in Figs. 4(a)–(c) and 5(a)–(c), respec-

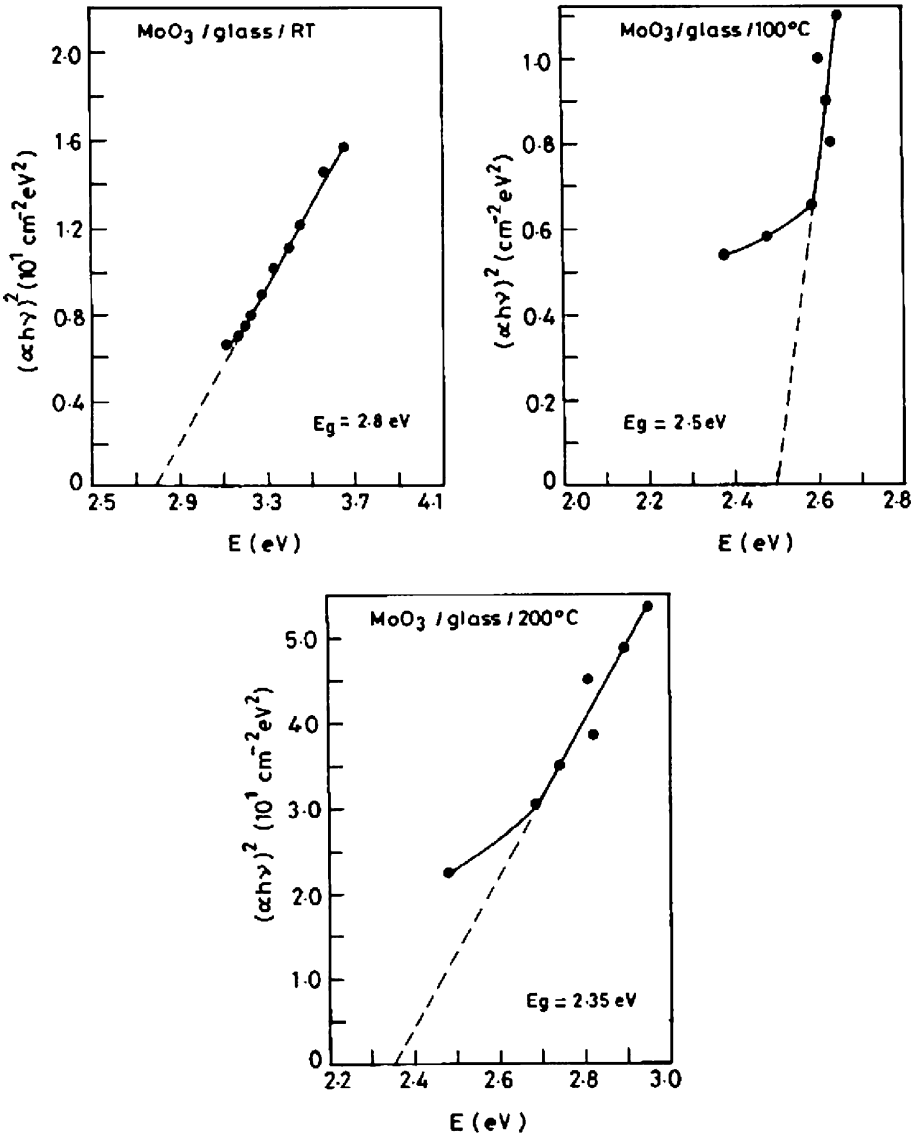

Fig. 8. Energy band gap graph of MoO_3 films on glass substrate at different substrate temperatures.

tively. The SEM images clearly show that the electron beam evaporated MoO_3 films are homogeneous, uniform and crack free surfaces. It is obvious that the growth conditions and methods have a strong influence on the surface morphology of the MoO_3 films. The SEM pictures of MoO_3 films deposited at various T_{sub} supports the correlation of the substrate temperature with change in adatom mobility.

Fig. 4(a) shows the SEM micrograph of the film on glass substrate at room temperature. It is having a very smooth morphology without any fragmentation features or topography contrast, which indicates the amorphous nature of the films. The improvement in crystallinity of the film occurs mainly by the coalescence of neighbouring crystallites (of nanometer size) driven by the thermal energy acquired from the heating process (T_{sub}). Rearrangement and alignment of the atoms are needed for initiating crystal growth, which are not favoured when the films are deposited on glass substrates at room temperature, because of the amorphous nature and non availability of thermal energy (room temperature) for atomic movement. Whereas some small grains are observed in micrograph (Fig. 5(a)), enumerated the crystalline nature of the films deposited on FTO substrates at RT. This is also identified from the XRD pattern (Fig. 2(a)). As discussed previously in X-ray diffraction analysis, the crystallization starts in the film grown at 100 °C (T_{sub}) on glass substrates. The increase in grain size and the origination of crystallization of films on glass substrate at $T_{sub} = 100$ °C are clearly observed in SEM micrograph (Fig. 4(b)). It is observed that the films are having whisker-like structure and arranged almost independent of clusters. The structure possesses a very high surface-to-volume ratio. But in the case of the films deposited on FTO substrates at the same condition (Fig. 5(b)), they show pearl like structure with platelets piled one over the other which corresponds to a layered structure. The needle-like crystallites were observed in the micrographs (Figs. 4(c) and 5(c)) for the films deposited at higher substrate temperature (200 °C). Formation of such needle-like morphology was observed by Comini et al. [22] for the RF sputtered MoO_3 films, which are subsequently post annealed at 800 K. Julien et al. [23] also reported that,

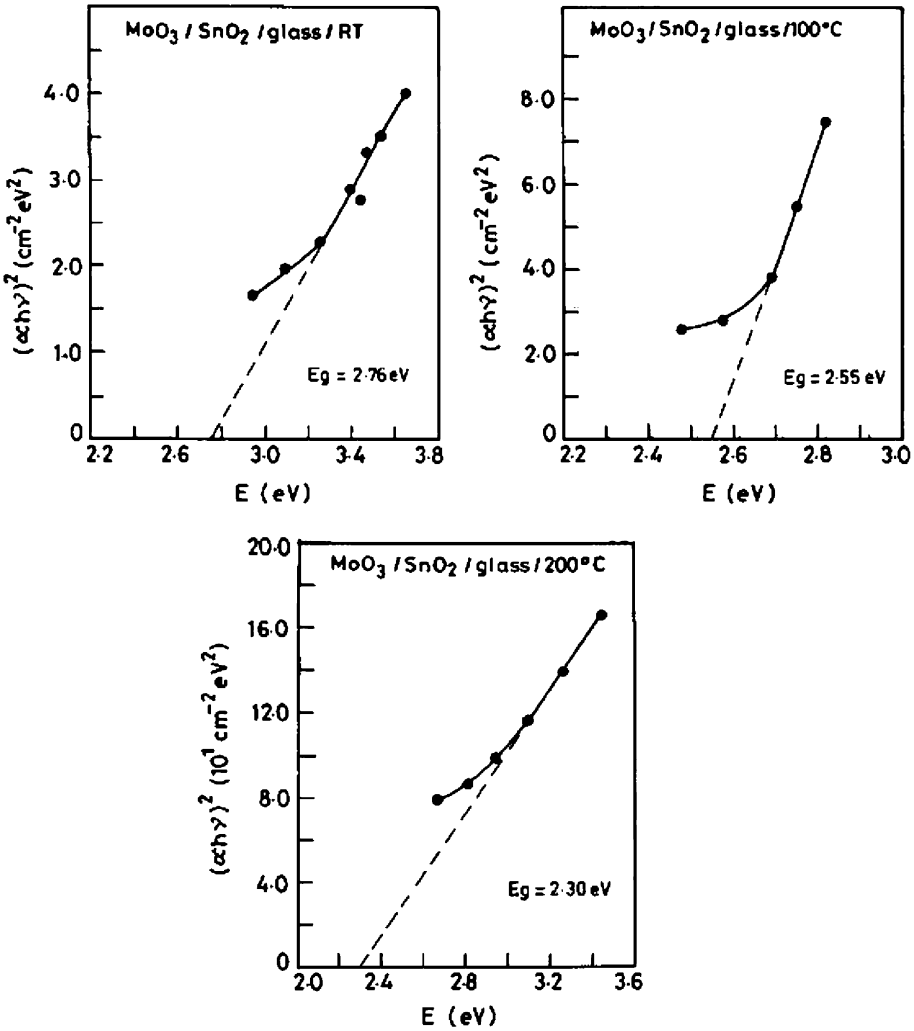

Fig. 9. Energy band gap graph of MoO_3 films on SnO_2:F substrate at different substrate temperatures.

needle-like elongated microcrystallites for the films deposited on Si substrates at 250 °C by flash evaporation technique. The different morphological micrographs of SEM showed the improvement of crystallinity of the films with various substrates and substrate temperatures. The change in surface morphology with different substrate temperatures is mainly due to the realization of different surface energy leading to crystallites of varying crystalline nature and size. Lower substrate temperature results in low surface migration of adatoms while too high substrate temperature causes the adatoms to re-evaporate from the film surface.

3.4. Optical studies

The influence of substrate temperature on the optical transmittance of MoO_3 films deposited on glass and FTO substrates was studied in the wavelength range between 300 and 1100 nm using HITACHI-3400 UV–Vis-NIR spectrophotometer and the recorded spectra are shown in Figs. 6 and 7, respectively. As can be seen from the spectra, samples deposited at lower substrate temperature ($T_{sub} = RT$) on glass and SnO_2:F substrates have higher transmittance in the range of about 95% and 91%, respectively. This clearly shows the transparent nature of the films. A broad absorption band was observed in the visible region of the spectrum and also the transmission threshold shifted towards higher wavelength side with increasing substrate temperature. It is worth noting that the coloration of the films is associated with the absorption edge shift [23]. The variations in transmission are mainly due to interference phenomena. Colored interference patterns are common for optically transparent film by naked eye. Thickness of the films was calculated from the interference pattern. The thickness of optimized MoO_3 films deposited at RT, 100 °C and 200 °C are 0.55, 1.32 and 1.80 μm, respectively. It is observed that the films deposited at 30 °C are light gray in color and transparent, whereas the films are deep blue color, when the films are grown at higher T_{sub} ($\geqslant$100 °C). As a result, various degrees of coloration occurred. It is concluded that the MoO_3 films prepared in the present work having perfect electrochromic nature.

The fundamental absorption edge of semiconductors corresponds to the threshold for charge transitions between the highest nearly filled band and the lowest nearly empty band. The absorption is very small for photon energy much less than the energy gap and increases significantly for higher photon energies. The intrinsic absorption edge of the films can be evaluated and discussed in terms of the direct interband transition. Thus, the plot $(\propto h\nu)^2$ versus E, called 'Tauc plot', is expected to show a linear behaviour in the higher energy region which corresponds to a strong absorption near the absorption edge. Extrapolating the linear portion of this straight line to zero absorption edge resulted the optical energy band gap, E_g of the films. The band gap graphs ($(\propto h\nu)^2$ versus E) of the MoO_3 films on glass and FTO substrates are shown in Figs. 8 and 9, respectively. It emphasized that the films are having direct band gap. The evaluated optical energy band gap of MoO_3 films prepared on glass substrates at RT, 100° and 200 °C, are 2.80, 2.50 and 2.35 eV, respectively. While, the band gap varied as 2.76, 2.55 and 2.30 eV for the films prepared on FTO substrates at RT, 100° and 200 °C, respectively. The graphical representation of variation in optical energy band gap values of MoO_3 films with increasing substrate temperature is shown in Fig. 10. Increasing the substrate temperature yields slight shrinkage in optical band gap. The slight band gap shrinkage is attributed primarily to the Moss–Burstein shift in semiconductors. The decreasing of energy band gap is due to oxygen ion vacancies, which are positively charged structural defects able to capture one or two electrons. The oxygen vacancies occupied by electrons act as donor centers whose level lie close to valance band, which are responsible for broad band absorption [24,25]. These donor centers are in the forbidden gap and form a narrow donor band at about 0.3 eV below the conduction band [26]. This is attributed to the excitation of trapped electrons into the conduction band. The band gap values derived from optical absorption studies are in accordance with the reported literatures [2,17,27,28]. The decrease in band gap is owing to the formation of more oxygen ion vacancies in the films. Julien et al. [23] reported the band gap of MoO_3 films deposited at room temperature is 3.37 eV, while it decreases to 2.80 eV for the films deposited at 300 °C. They also suggested that the decrease in band gap with increasing substrate temperature due to the formation oxygen-ion vacancies. Bouzidi et al. [17] observed the E_g values from 3.14 to 3.34 eV. At the substrate temperature of 200 °C,

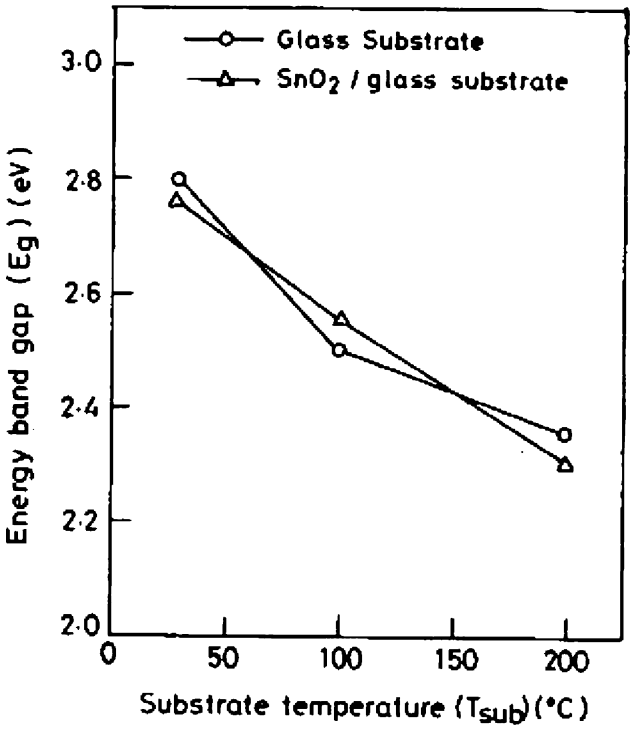

Fig. 10. Variation of energy band gap of MoO_3 films with respect to substrate temperatures.

the energy gap is 3.3 eV, and increases slightly up to 3.34 eV for $T_{sub} = 250$ °C. Above this substrate temperature, the E_g value decrease until 3.14 eV at 300 °C. Hence, they conclude that the increasing of E_g value is attributed to the partial filling of oxygen vacancies, whereas the decreasing of energy gap is due to the formation of oxygen-ion vacancies. Also we have observed from the particle induced X-ray emission spectroscopic analysis [29], the decreasing of oxygen concentration with increasing substrate temperature, which reconciled the formation of oxygen-ion vacancies in the films. Hence the results obtained in the present work are well correlated with our earlier reported work.

4. Conclusions

Thin films of MoO_3 were deposited by the electron beam evaporation technique on glass and FTO substrates in the temperature range 30–200 °C. The influence of substrates and temperature of substrates on the structural, surface and optical properties of the films is studied. It is observed that the control of deposition temperature promotes the film crystallinity. The structural studies reveal that the improvement in crystallinity depends on the nature of the substrate and substrate temperatures. The XRD patterns clearly show the preferred growth along $\langle 1\,1\,0\rangle$ orientation combine with $\langle 0k0\rangle$ orientations correspond to the orthorhombic phase of molybdenum oxide ($\propto$-MoO_3) thin films. Raman spectra show that for polycrystalline MoO_3 films the MoO_6 octahedra are progressively connected and the structural reorganization is mainly observed for the Mo–O stretching mode that is associated with the unique character of the layered structure of orthorhombic MoO_3. The needle-like crystallites are observed in the films prepared at 200 °C, which also confirm the layered nature of the films. The absorption edge shifted towards the higher wavelength region with increasing substrate temperature may be attributed to the coloration effect on the films. The optical studies reveal that the variation of band gap is dependent on the preparation conditions, which in turn influences the crystallinity and the morphology of the films. Based on these results, it may be concluded that α-MoO_3 films deposited at lower temperature on FTO substrates have layered structure, which can be effectively used for developing efficient electrochromic devices.

Acknowledgements

One of the authors R. Sivakumar gratefully acknowledges the Council of Scientific and Industrial Research (CSIR, New Delhi), Government of India, for having awarded the Senior Research Fellowship (SRF).

References

[1] K. Hinokuma, A. Kishimoto, T. Kudo, J. Electrochem. Soc. 141 (1994) 876.
[2] C.G. Granqvist, Handbook of Inorganic Electrochromic Materials, Elsevier, Amsterdam, 1995.
[3] S.S. Sunu, E. Prabu, V. Jayaraman, K.I. Gnanasekar, T. Gnanasekaran, Sens. Actuators, B 94 (2003) 189.
[4] C.M. Lampert, Sol. Energ. Mater. 11 (1984) 1.
[5] H. Ohtsuka, Y. Sakurai, Solid State Ionics 144 (2001) 59.
[6] C. Julien, G.A. Nazri, J.P. Guesdon, A. Gorenstein, A. Khelfa, O.M. Hussain, Solid State Ionics 73 (1994) 319.
[7] P.G. Dickens, S. Crouch-Baker, M.T. Weller, Solid State Ionics 18–19 (1986) 89.
[8] N. Sotani, K. Eda, M. Sadamatu, S. Takagi, Bull. Chem. Soc. Jap. 62 (1989) 903.
[9] K. Kalatsis, Y.X. Li, W. Wlodarski, K. Kalantar-zadesh, Sens. Actuators, B 77 (2001) 478.
[10] Shaoqin Liu, Qibin Zhang, Erkang Wang, Shaojun Dong, Electrochem. Commun. 1 (1999) 365.
[11] K. Srinivasa Rao, K.V. Madhuri, S. Uthanna, O.M. Hussain, C. Julien, Mater. Sci. Eng. B 100 (2003) 79.
[12] C. Imawan, H. Steffes, F. Solzbacher, E. Obermeier, Sens. Actuators, B 78 (2001) 119.
[13] K.V. Madhuri, B.S. Naidu, O.M. Hussain, M. Eddrief, C. Julien, Mater. Sci. Eng. B 86 (2001) 165.
[14] R.F. Bunshah, Thin Solid Films 80 (1981) 255.
[15] C. Julien, L. El-Farh, M. Balkanski, O.M. Hussain, G.A. Nazri, Appl. Surf. Sci. 65–66 (1993) 325.
[16] A. Abdellaoui, G. Leveque, A. Donnadieu, A. Bath, B. Bouchikhi, Thin Solid Films 304 (1997) 39.
[17] A. Bouzidi, N. Benramdane, H. Tabet-Derraz, C. Mathieu, B. Khelifa, R. Desfeux, Mater. Sci. Eng. B 97 (2003) 5.
[18] B.D. Cullity, Elements of X-ray diffraction, Philippines copy right, Addision-Wesley publishing company, Inc., 1978.
[19] G.A. Nazri, C. Julien, Solid State Ionics 53–56 (1992) 376.
[20] I.R. Beattie, T.R. Gilson, J. Chem. Soc. A (1969) 2322.
[21] K. Gesheva, A. Szekeres, T. Ivanova, Sol. Energ. Mater. Sol. Cells 76 (2003) 563.
[22] E. Comini, G. Faglia, G. Sberveglieri, C. Cantalini, M. Passacantando, S. Santucci, Y. Li, W. Wlodarski, W. Qu, Sens. Actuators, B 68 (2000) 168.
[23] C. Julien, A. Khelfa, O.M. Hussain, G.A. Nazri, J. Cryst. Growth 156 (1995) 235.
[24] V.K. Sabhapathi, O.M. Hussain, P.S. Reddy, K.T.R.K. Reddy, S. Uthanna, B.S. Naidu, P.J. Reddy, Phys. Status Solidi A 148 (1975) 167.
[25] M. Anwar, C.A. Hogarth, Int. J. Electron. 67 (1987) 567.
[26] G.S. Nadkarni, J.G. Simmons, J. Appl. Phys. 41 (1970) 545.
[27] Y. Hiruta, M. Kitao, S. Yamada, Jpn. J. Appl. Phys. 23 (1984) 1624.
[28] R.J. Colton, A.M. Guzman, J.W. Rabalais, Acc. Chem. Res. 11 (1978) 170.
[29] R. Sivakumar, V. Vijayan, V. Ganesan, M. Jayachandran, C. Sanjeeviraja, Smart. Mater. Struct. 14 (2005) 1204.